DOI: 10.1002/anie.201206316

Photosystem II Structure

Rationalizing the 1.9 Å Crystal Structure of Photosystem II—A Remarkable Jahn–Teller Balancing Act Induced by a Single Proton Transfer**

Phillip Gatt, Simon Petrie, Rob Stranger, and Ron J. Pace**

Green plants and algae oxidize water to molecular oxygen in photosystem II (PS II) within a calcium/tetramanganese site known as the water-oxidizing complex (WOC). Oxygen is generated by the WOC in a four-electron process involving a series of intermediate states (S states, labeled $S_0 \ldots S_4$) of increasingly higher mean oxidation level.[1] Over the past decade, X-ray crystallographic (XRD) structures of PS II at progressively improved resolution[2] have revealed much detail of the WOC. At present, only PS II from thermophilic cyanobacteria has been crystallized for XRD study and the enzyme is presumed to be in the dark stable S_1 state. The first PS II structure (at 3.5 Å resolution) to resolve side chain positions was presented by Barber and co-workers.[2c] Consistent with subsequent studies at higher resolution, it revealed the compact Mn_3Ca "cube" structure of the WOC connected more distantly to a single Mn, referred to as the "dangler". More recent improved structures at 3.0 Å and 2.9 Å,[2d,e] substantially clarified the metal- and protein-supplied ligand positions within the WOC, but were still of insufficient resolution to reveal the positions of bridging oxo groups and water molecules (including the substrate water molecules). Finally, Umena et al.,[2f] using a new crystallization method, produced an atomic resolution structure at 1.9 Å, the most resolved to date. Despite this remarkable achievement, revealing, for the first time, the positions of bridging O atoms within the Mn_4Ca core of the WOC, aspects of the new structure have been met with scepticism.[3,4] Central concerns over this structure involve 1) the identity and unexpected placement of the O(5) moiety (Figure 1), which appears to be either a weakly bound oxo, hydroxo, or water ligand at distances of 2.4–2.7 Å from four of the metal atoms in the WOC, and 2) the disparity in some key metal–metal distances when compared with earlier, high-precision extended X-ray absorption fine structure (EXAFS) results[5,6] and the previous lower-resolution XRD structures (see Table 1). Although the Mn EXAFS data do not unambiguously assign the individual near (less than 3 Å) metal–metal distances within the cluster, they clearly indicate that two Mn-Mn vectors of a magnitude of approximately 2.7 Å exist within the functional WOC in the S_1 and S_2 states. These are totally consistent with the Mn1-Mn2 and Mn2-Mn3 distances of 2.65 Å and 2.70 Å in the 2.9 Å resolution XRD structure, but are significantly shorter than the corresponding Mn-Mn distances of 2.80 Å and 2.90 Å seen in the 1.9 Å resolution XRD structure.

Table 1: Metal–metal distances from EXAFS studies,[5,6] and the Loll et al.[2d,e] and Umena et al.[2f] XRD structure determinations for the PS II WOC, compared with the model geometries obtained from our DFT calculations (Opt).

Parameter[a]	EXAFS[b]	Loll[b] 2.9[c]	Opt[b]	Umena[b] 1.9[c]	Opt[b]
r[Mn(1)-Mn(2)]	2.69–2.77	2.65	2.794	2.80	2.897
r[Mn(2)-Mn(3)]	2.69–2.77	2.70	2.851	2.90	2.895
r[Mn(1)-Mn(3)]		3.29	3.625	3.30	3.425
r[Mn(3)-Mn(4)]		3.25	3.372	2.94	3.035
r[Mn(1)-Mn(4)]		5.43	5.331	4.98	5.088
r[Ca-Mn(1)]		3.38	3.520	3.48	3.376
r[Ca-Mn(2)]		3.22	3.205	3.33	3.185
r[Ca-Mn(3)]		3.29	3.317	3.43	3.484
r[Ca-Mn(4)]		4.63	4.043	3.80	3.817
r[O(5)-Mn(1)]		–		2.60	2.641
r[O(5)-Mn(3)]		–		2.40	2.615
r[O(5)-Mn(4)]		–		2.47	2.605
r[O(5)-Ca]		–		2.80	2.711

[a] Refer to Figure 1 for Mn atom numbering. [b] in Å. [c] Resolution of the XRD structure in Å.

The discrepancies between the XRD and EXAFS data have led some to suggest[3,4,7] that the crystal structures generally, and the 1.9 Å resolution structure in particular, have undergone photoreduction of the Mn atoms during data collection, increasing the Mn^{II} content and distorting the cluster from the functional S_1 state to as low as S_{-3}. This is despite the fact that in the later studies great pains were taken to minimize such X-ray exposure. The claims of photoreduction arise from two sources—monitoring the effects of progressive X-ray exposure using Mn EXAFS[4,7] and high level computational modeling of the WOC cluster.[3] Although the 2.9 Å structure is quite consistent with the results from EXAFS (including one-dimensional oriented Mn

[*] P. Gatt, Dr. S. Petrie, Prof. R. Stranger, Prof. R. J. Pace
Research School of Chemistry, Australian National University
Canberra ACT 0200 (Australia)
E-mail: rob.stranger@anu.edu.au
ron.pace@anu.edu.au

[**] R.S. and R.J.P. gratefully acknowledge financial assistance from the Australian Research Council. We also acknowledge the generous provision of supercomputing time on the platforms of the NCI (National Computational Infrastructure) Facility in Canberra, Australia, which is supported by the Australian Commonwealth Government. We also thank Richard Terrett for assistance in the preparation of the manuscript figures.

Supporting information for this article (experimental details) is available on the WWW under http://dx.doi.org/10.1002/anie.201206316.

© 2012 Wiley-VCH Verlag GmbH & Co. KGaA, Weinheim

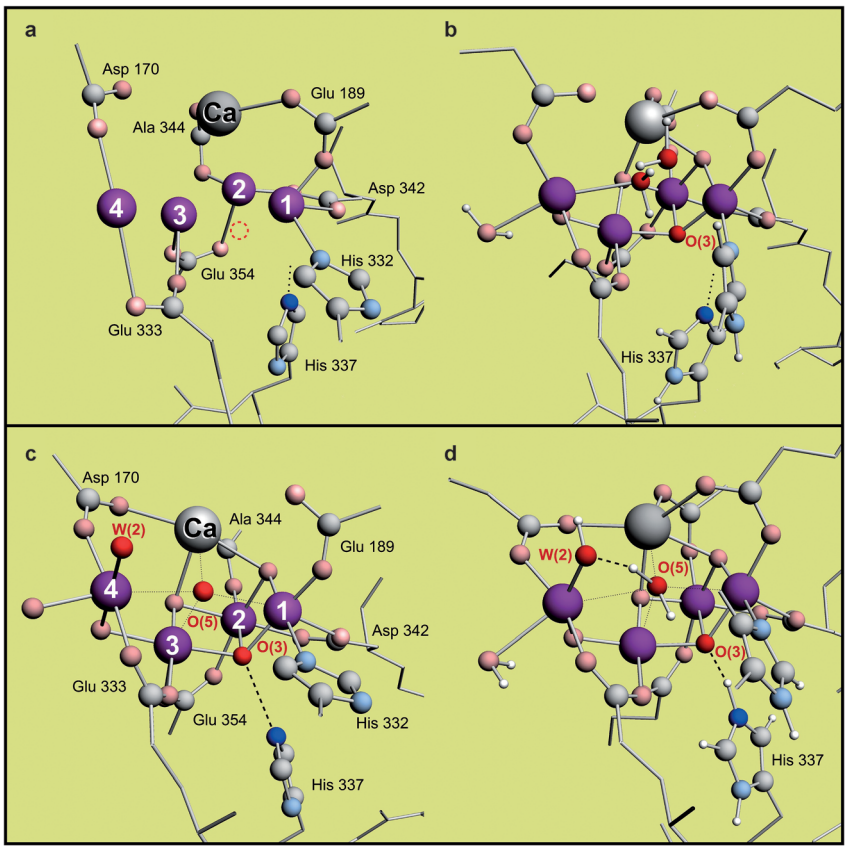

Figure 1. The experimental (a) and modeled (b) WOC region geometries for the 2.9 Å PS II structure type (purple spheres = Mn atoms; for the full model see the Supporting Information, Figure S1). Extra components (oxygen species) are present in the modeled structure which are not resolved at 2.9 Å in the XRD structure (see text). The inferred position of O(3), which is a μ_3-oxo bridge, is indicated in the XRD structure (dashed circle in a). The N_τ of His337 points away from this oxo bridge in both structures, consistent with the absence of any H-bonding interaction. c,d) The corresponding geometries for the 1.9 Å PS II structure type (for the full model see Figure S2). The orientation of His337 and the O(3)-His337 distance are now consistent with H-bonding being present, as explicitly included in the model (dashed line in (d). The experimental W(2) and O(5) positions are well reproduced in the model, with W(2) now an OH^- group (H_2O in b). Both computational structures (b) and (d) have identical formal total charge (0) and mean Mn oxidation state (+3.0; water molecules on Ca have been removed for clarity). They are single-proton shifted tautomers of each other (from W(2) to His337, see text).

EXAFS studies on plant PS II membranes),[5] recent computational studies[3,8a,e,14] on the 1.9 Å WOC structure suggest that the Mn–Mn distances are generally too long for the cluster topology and mean Mn oxidation level (average +3.5) assumed for the S_1 state by those workers.

To rationalize the XRD results and provide insight into the mechanism of oxygen evolution in PS II, several groups have used density functional theory (DFT) to explore models of the WOC.[3,8,10,14,15] Of late, these have involved large-scale calculations including the metal centers and surrounding protein components, with structures constrained at their peripheries by the available XRD data.[3,8a,13,14] Crucial in these calculations is an assumed mean oxidation level for the Mn ions, which has long been known to be significantly above +2.0 in the functional enzyme. From spectroscopic data, the mean level in the S_1 state must be +3.0 or +3.5. We have labeled these alternatives the "low" and "high" oxidation paradigms. The high oxidation paradigm (i.e. $Mn^{III}{}_2Mn^{IV}{}_2$) has been favored by most computational groups, based on spectroscopic (principally X-ray absorption near edge structure (XANES), electron paramagnetic resonance (EPR) evidence.[10] However, this largely empirical assignment relies heavily on comparisons with model systems, none of which are precise analogues of the actual WOC Mn environment. Recently, we have shown, using a new time-dependent DFT approach, that when the metal-ligand environments are properly accounted for, the available Mn XANES data are most consistent with the low oxidation paradigm.[8b,c] An extensive re-examination of other spectroscopic data also supports this conclusion.[8d] Further, a very recent study by Dismukes and co-workers,[9] employing a totally different approach that simply counts the electrons removed from four Mn^{II} ions during photoassembly of the functional enzyme (from the apo-protein), clearly establishes the validity of the low oxidation paradigm. This raises the possibility that the assumed Mn oxidation levels in the functional enzyme may hold the key to understanding the apparent discrepancies in the XRD and EXAFS data of PS II.

To address this issue we have undertaken large scale (approximately 200 atom) full DFT modeling of the WOC region employing the highest feasible levels of theory, including explicit characterization of the peptide sequence His332–Ala344 on the D1 reaction-center polypeptide, which dominates the immediate environs of the Mn_4Ca core (see Supporting Information). This approach has been applied to both the 2.9 Å (Loll) and 1.9 Å (Umena) structures. These results, together with the corresponding XRD portions, are shown in Figure 1 and in the Supporting Information (full model structures). The mean Mn redox level is +3.0 for both structures (low oxidation paradigm S_1). An important difference is that in the 1.9 Å structure, His337 is directly orientated towards the μ_3-oxo bridge (O(3)) and, as our recent calculations showed,[8a] is close enough ($O(3)–N_{His337} = 2.67$ Å) to engage in H-bonding (Figure 1). In the 2.9 Å structure however, His337 is unlikely to be involved in H-bonding as it is further away and not orientated towards the inferred position of the μ_3-oxo bridge.

In the 2.9 Å model structure, our large scale calculations reveal that the oxidation state pattern for Mn1–Mn4 is III/IV/III/II, in agreement with our earlier calculations on smaller scale models for the low oxidation paradigm S_1 state.[15] The calculated metal–metal distances listed in Table 1 are all close to the XRD values and consistent with the EXAFS data. The

© 2012 Wiley-VCH Verlag GmbH & Co. KGaA, Weinheim

Mn1-Mn2 and Mn2-Mn3 vectors are short, while the Mn3-Mn4 is long. The short Mn–Mn distances arise because Mn2 is in the IV oxidation state, which allows short di-μ-oxo bridged vectors to Mn1 and Mn3, without Jahn–Teller "frustration" which would be present if Mn2 was in the III oxidation state. The long Mn3-Mn4 distance is a consequence of a single oxo bridge between these ions with both terminal oxygen groups on Mn4 being water molecules. This arrangement favors the II oxidation state for Mn4 in the S_1 state and we have recently highlighted the importance of this for redox accumulation within the cluster.[8f]

If Mn2 acquires the III oxidation state, the vectors to Mn1 and/or Mn3 must elongate as a bridging oxo group which connects these metals with Mn2 is now always located on a Jahn–Teller axis of Mn2. If the Jahn–Teller distortion is along one of the μ_2-oxo bridges, then either the Mn1-Mn2 or Mn2-Mn3 vectors will elongate. However, if the distortion is along the μ_3-oxo bridge (O(3) in Figure 1), then both the Mn1-Mn2 and Mn2-Mn3 distances will be elongated. This is precisely the circumstance in our model of the 1.9 Å structure (see Table 1), where the Mn oxidation state pattern is now III/III/III/III instead of III/IV/III/II present in the 2.9 Å structure. Specifically, our calculations show that it is the Mn2 bond to the μ_3-oxo bridge that weakens as a result of the Jahn–Teller distortion and H-bonding to His337. Also, the Mn3-Mn4 vector shortens as a consequence of Mn4 now being in the III state. Remarkably, as depicted in Scheme 1, this total

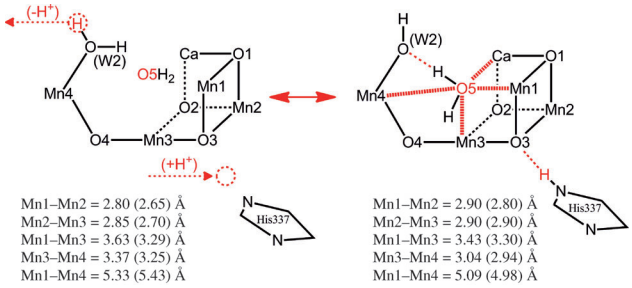

Scheme 1. Diagram illustrating the interconversion of structures modeling the 2.9 Å (left) and 1.9 Å resolution (right) XRD structures, as mediated by proton transfer from a water molecule (W2) to His337. Bond lengths listed are those of our computational models, with the corresponding XRD values in parentheses.

change is triggered by a single proton relocation from a terminal water molecule on Mn4 to the N_τ of His337. This allows His337 to engage in H-bonding with the μ_3-oxo bridge (an interaction strongly inferred from the 1.9 Å structure) which weakens its bond with Mn2, converting it from the IV to III oxidation state and forcing the Mn1-Mn2 and Mn2-Mn3 vectors to lengthen. As is apparent from Figure 1 and Table 1, our calculated model is in very good agreement with the 1.9 Å structure with all Mn–Mn distances within 0.13 Å, all Mn–Ca distances within 0.15 Å, and all metal–O(5) distances within 0.22 Å of the XRD values.

In addition to these observations, our computational model now reveals, for the first time, the nature of the anomalous central O(5) moiety and its unusual placement in the 1.9 Å structure. The position of this group has proven very difficult to rationalize[3,8e,14] because it is roughly equidistant from several metals, with no strong interaction with any of them. To date, it has been modeled as an oxo or hydroxo group with Mn–O distances significantly shorter than those seen experimentally, a consequence of the high mean Mn oxidation levels assumed in the calculations. From Scheme 1 and Figure 2, our modeling shows that O(5) is a water ligand,

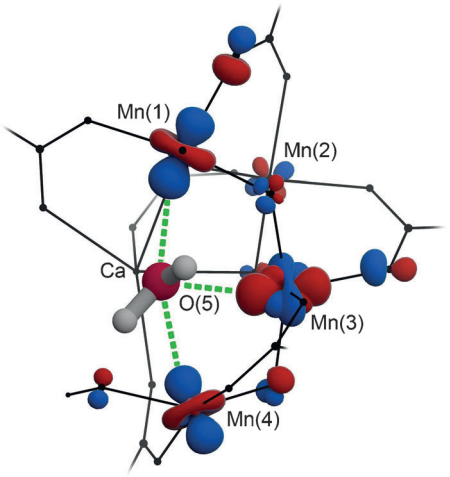

Figure 2. Local region of the O(5) moiety, modeled as a water molecule, in the computational model of the 1.9 Å XRD structure. Shown are the d orbitals of Mn involved in the Jahn–Teller elongation on Mn1, Mn3, and Mn4, which all point directly towards the O(5) atom and account for the anomalously long distances of O(5) to these metals.

delicately "balanced" upon a "Jahn–Teller tripod" in the cleft region of the cluster defined by Mn1, Mn3, Mn4, and Ca, and H-bonded to the now terminal hydroxide group on Mn4, a result of the proton re-location noted above. The fact that this ligand is positioned at the convergence of Jahn–Teller axes on Mn1, Mn3, and Mn4 accounts for the anomalously long bond distances to these metals. Further, the position of O(5) is consistent with the location we have earlier identified for one of the two substrate water molecules.[15b,c]

The 1.9 Å structure is an extremely important advance in our understanding of PS II and the WOC in particular. Because our calculations indicate that the O(5) group is an obvious candidate for a substrate species, it is vital that the relevance of this structure to the functional state of the enzyme be established. Our studies herein show that the two best resolved structures now available are both computationally consistent with each other and with independent data (Mn EXAFS). Importantly, this result has been achieved without the need to invoke photoreduction of the Mn centers. The 2.9 Å and 1.9 Å XRD structure forms are simply and remarkably single-proton tautomers of each other, having the same overall average Mn oxidation level of +3.0 but a different sequence of Mn oxidation states, III/IV/III/II and III/III/III/III, respectively. Further, the mean oxidation state in both model structures is in agreement with the value obtained from the recent experimental study of Dismukes and co-workers.[9] The two tautomers are only separated energetically by

 © 2012 Wiley-VCH Verlag GmbH & Co. KGaA, Weinheim

approximately 40 kJ mol^{-1}, in favor of the 1.9 Å structure. This may well have functional relevance in the enzyme mechanism or photoassembly process, as it highlights the significance of His337, previously known from PS II mutational studies to be functionally important in its assembly, possibly as an H-bond donor.[16] The keys to this outcome are that the mean Mn oxidation level in the S_1 state is +3.0 not +3.5, as we have recently shown,[8a,c,d,e] and that N_τ on His337 must be deprotonated in the 2.9 Å structure and protonated in the 1.9 Å structure. In fact, it has proven impossible for us and others to rationalize the detail of the 1.9 Å structure in particular, in terms of the higher oxidation state.[3,8e,14] While an argument could be made implying that the crystal structures are indeed photoreduced, this essentially random process would need to occur systematically and uniformly in two crystal matrices of essentially the same PS II material, producing two distinctly resolved outcomes for the WOC region and maintaining a coherently identifiable distinction (in both cases) between the two monomers (A and B) within the crystallized dimer. This strikes us as very improbable.

Received: August 7, 2012
Published online: October 26, 2012

Keywords: density functional calculations · photosystem II · water-oxidizing complex · water splitting · X-ray diffraction

[1] K. Satoh, T. Wydrzynski, Govindjee, *Photosystem II: The Light Driven Water: Plastoquinone Oxidoreductase*, Springer, Dordrecht, **2005**, pp. 11 – 22.

[2] a) A. Zouni, H.-T. Witt, J. Kern, P. Fromme, N. Krauss, W. Saenger, P. Orth, *Nature* **2001**, *409*, 739 – 743; b) N. Kamiya, J.-R. Shen, *Proc. Natl. Acad. Sci. USA* **2003**, *100*, 98 – 103; c) K. N. Ferreira, T. M. Iverson, K. Maghlaoui, J. Barber, S. Iwata, *Science* **2004**, *303*, 1831 – 1838; d) B. Loll, J. Kern, W. Saenger, A. Zouni, J. Biesiadka, *Nature* **2005**, *438*, 1040 – 1044; e) A. Guskov, J. Kern, A. Gabdulkhalov, M. Broser, A. Zouni, W. Saenger, *Nat. Struct. Mol. Biol.* **2009**, *16*, 334 – 342; f) Y. Umena, K. Kawakami, J.-R. Shen, N. Kamiya, *Nature* **2011**, *473*, 55 – 60.

[3] a) S. Luber, I. Rivalta, Y. Umena, K. Kawakami, J.-R. Shen, N. Kamiya, G. W. Brudvig, V. Batista, *Biochemistry* **2011**, *50*, 6308 – 6311; b) P. E. M. Siegbahn, *ChemPhysChem* **2011**, *12*, 3274 – 3280; c) W. Ames, D. A. Pantazis, V. Krewald, N. Cox, J. Messinger, W. Lubitz, F. Neese, *J. Am. Chem. Soc.* **2011**, *133*, 19743 – 19757; d) A. Galstyan, A. Robertazzi, E. W. Knapp, *J. Am. Chem. Soc.* **2012**, *134*, 7442 – 7449.

[4] A. Grundmeier, H. Dau, *Biochim. Biophys. Acta Bioenerg.* **2012**, *1817*, 88 – 105.

[5] M. Haumann, C. Müller, P. Liebisch, L. Iuzzolino, J. Dittmer, M. Grabolle, T. Neisius, W. Meyer-Klaucke, H. Dau, *Biochemistry* **2005**, *44*, 1894 – 1908.

[6] J. Yano, Y. Pushkar, P. Glatzel, A. Lewis, K. Sauer, J. Messinger, U. Bergmann, V. Yachandra, *J. Am. Chem. Soc.* **2005**, *127*, 14974 – 14975.

[7] J. Yano, J. Kern, K.-D. Irrgang, M. J. Latimer, U. Bergmann, P. Glatzel, Y. Pushkar, J. Biesiadka, B. Loll, K. Sauer, J. Messinger, A. Zouni, V. K. Yachandra, *Proc. Natl. Acad. Sci. USA* **2005**, *102*, 12047 – 12052.

[8] a) S. Petrie, P. Gatt, R. Stranger, R. J. Pace, *Phys. Chem. Chem. Phys.* **2012**, *14*, 4651 – 4657; b) A. R. Jaszewski, R. Stranger, R. J. Pace, *Phys. Chem. Chem. Phys.* **2009**, *11*, 5634 – 5642; c) A. R. Jaszewski, S. Petrie, R. J. Pace, R. Stranger, *Chem. Eur. J.* **2011**, *17*, 5699 – 5713; d) R. J. Pace, L. Jin, R. Stranger, *Dalton Trans.* **2012**, *41*, 11145 – 11160; e) S. Petrie, P. Gatt, R. Stranger, R. J. Pace, *Phys. Chem. Chem. Phys.* **2012**, *14*, 11333 – 11343; f) R. J. Pace, R. Stranger, S. Petrie, *Dalton Trans.* **2012**, *41*, 7179 – 7189.

[9] D. R. J. Kolling, N. Cox, G. M. Ananyev, R. J. Pace, G. C. Dismukes, *Biophys. J.* **2012**, *103*, 313 – 322.

[10] P. Gatt, R. Stranger, R. J. Pace, *J. Photochem. Photobiol. B* **2011**, *104*, 80 – 93.

[11] E. M. Sproviero, J. P. McEvoy, J. A. Gascon, G. W. Brudvig, V. S. Batista, *Photosynth. Res.* **2008**, *97*, 91 – 114.

[12] I. Rivalta, G. W. Brudvig, V. S. Batista, *Curr. Opin. Chem. Biol.* **2012**, *16*, 11 – 18.

[13] P. E. M. Siegbahn, *Acc. Chem. Res.* **2009**, *42*, 1871 – 1880.

[14] a) P. E. M. Siegbahn, *Phys. Chem. Chem. Phys.* **2012**, *14*, 4849 – 4856; b) M. Kusunoki, *J. Photochem. Photobiol.* **2011**, *104*, 100 – 110; c) T. Saito, S. Yamanaka, K. Kanda, H. Isobe, Y. Takano, Y. Shigeta, Y. Umena, K. Kawakami, J.-R. Shen, N. Kamiya, M. Okumura, M. Shoji, Y. Yoshioka, K. Yamaguchi, *Int. J. Quantum Chem.* **2012**, *112*, 253 – 276; d) S. Yamanaka, T. Saito, K. Kanda, H. Isobe, Y. Umena, K. Kawakami, J.-R. Shen, N. Kamiya, M. Okumura, H. Nakamura, K. Yamaguchi, *Int. J. Quantum Chem.* **2012**, *112*, 321 – 343; e) D. A. Pantazis, W. Ames, N. Cox, W. Lubitz, F. Neese, *Angew. Chem.* **2012**, *124*, 10074 – 10079; *Angew. Chem. Int. Ed.* **2012**, *51*, 9935 – 9940.

[15] a) S. Petrie, R. Stranger, P. Gatt, R. J. Pace, *Chem. Eur. J.* **2007**, *13*, 5082 – 5089; b) S. Petrie, R. Stranger, R. J. Pace, *Angew. Chem.* **2010**, *122*, 4329 – 4332; *Angew. Chem. Int. Ed.* **2010**, *49*, 4233 – 4236; c) S. Petrie, R. Stranger, R. J. Pace, *Chem. Eur. J.* **2010**, *16*, 14026 – 14042.

[16] R. J. Debus, *Biochim. Biophys. Acta Bioenerg.* **2001**, *1503*, 164 – 186.

 © 2012 Wiley-VCH Verlag GmbH & Co. KGaA, Weinheim